



**HAL**  
open science

# Evidence for a “metabolically inactive” inorganic phosphate pool in adenosine triphosphate synthase reaction using localized $^{31}\text{P}$ saturation transfer magnetic resonance spectroscopy in the rat brain at 11.7 T

Brice Tiret, Emmanuel Brouillet, Julien Valette

## ► To cite this version:

Brice Tiret, Emmanuel Brouillet, Julien Valette. Evidence for a “metabolically inactive” inorganic phosphate pool in adenosine triphosphate synthase reaction using localized  $^{31}\text{P}$  saturation transfer magnetic resonance spectroscopy in the rat brain at 11.7 T. *Journal of Cerebral Blood Flow and Metabolism*, 2016, 36 (9), pp.1513-1518. 10.1177/0271678X16657095 . cea-02155315

**HAL Id: cea-02155315**

**<https://cea.hal.science/cea-02155315>**

Submitted on 13 Jun 2019

**HAL** is a multi-disciplinary open access archive for the deposit and dissemination of scientific research documents, whether they are published or not. The documents may come from teaching and research institutions in France or abroad, or from public or private research centers.

L'archive ouverte pluridisciplinaire **HAL**, est destinée au dépôt et à la diffusion de documents scientifiques de niveau recherche, publiés ou non, émanant des établissements d'enseignement et de recherche français ou étrangers, des laboratoires publics ou privés.

# Evidence for a “metabolically inactive” inorganic phosphate pool in adenosine triphosphate synthase reaction using localized $^3\text{P}$ saturation transfer magnetic resonance spectroscopy in the rat brain at 11.7 T

Brice Tiret<sup>1,2</sup>, Emmanuel Brouillet<sup>1,2</sup> and Julien Valette<sup>1,2</sup>

## Abstract

With the increased spectral resolution made possible at high fields, a second, smaller inorganic phosphate resonance can be resolved on  $^3\text{P}$  magnetic resonance spectra in the rat brain. Saturation transfer was used to estimate *de novo* adenosine triphosphate synthesis reaction rate. While the main inorganic phosphate pool is used by adenosine triphosphate synthase, the second pool is inactive for this reaction. Accounting for this new pool may not only help us understand  $^3\text{P}$  magnetic resonance spectroscopy metabolic profiles better but also better quantify adenosine triphosphate synthesis.

## Keywords

Mathematical modelling, energy metabolism, adenosine triphosphate, pH, magnetic resonance spectroscopy

Received 26 February 2016; Revised 26 May 2016; Accepted 26 May 2016

## Introduction

Phosphorus ( $^3\text{P}$ ) magnetic resonance spectroscopy (MRS) can be used to non-invasively quantify metabolites involved in energy metabolism, such as adenosine triphosphate (ATP), phosphocreatine (PCr) and inorganic phosphate (Pi). It has been widely used to study muscles but also brain and liver (Befroy et al.<sup>1</sup> and references herein). In addition to the metabolic profile,  $^3\text{P}$  MRS has the added benefit of allowing the non-invasive measurement of pH.<sup>2</sup> Furthermore, saturation transfer experiments can be used to quantify reaction rates between exchanging pools<sup>3</sup> and can be of particular interest when studying brain metabolism together with other methods.<sup>4</sup>

At high magnetic fields, there is an increase in  $^3\text{P}$  spectral resolution that can help differentiate peaks that would otherwise overlap. Previous studies in the muscle have reported resonances between 5.1 and 5.3 ppm that could be attributed to a second pool of Pi (the main pool resonating at 4.9 ppm). These studies suggested that the alkaline pool of Pi may originate from

extracellular space,<sup>5</sup> blood<sup>6</sup> or mitochondrial space.<sup>7,8</sup> Other studies at lower fields have been trying to deconvolve the broad Pi peak into various number of pools and attribute them to specific cellular compartments in isolated brains.<sup>9–11</sup> A very recent study in the human brain<sup>12</sup> found the second Pi pool resonating at 5.24 ppm to be insensitive to selective inversion of PCr and  $\gamma$ -ATP,<sup>13</sup> suggesting the absence of chemical

<sup>1</sup>Commissariat à l'Energie Atomique et aux Energies Alternatives (CEA), Direction de la Recherche Fondamentale (DRF), Institut d'Imagerie Biomédicale (I2BM), Molecular Imaging Research Center (MIRCent), Fontenay-aux-Roses, France

<sup>2</sup>Centre National de la Recherche Scientifique (CNRS), Université Paris-Saclay, UMR 9199, Neurodegenerative Diseases Laboratory, Fontenay-aux-Roses, France

## Corresponding author:

Brice Tiret, Commissariat à l'Energie Atomique (CEA), Direction de la Recherche Fondamentale (DRF), Institut d'Imagerie Biomédicale (I2BM), Molecular Imaging Research Center (MIRCent), 18 route du Panorama, Fontenay-aux-Roses 92260, France.  
Email: brice.tiret@cea.fr

exchange with Pi and thus supporting the extra-cellular hypothesis.

The aim of this study was to combine high magnetic field (11.7 T) and spectroscopic localization to achieve good spectral resolution and test this hypothesis, i.e. characterize Pi pools (noted Pi<sub>4.9</sub> and Pi<sub>5.3</sub>) in the rat brain, including saturation transfer experiments to estimate the participation of each pool to ATP synthesis. We also evaluated how not accounting for the existence of this smaller pool of Pi could possibly result in biased estimation of ATP synthase reaction rate ( $k_{fATPase}$ ).

## Methods

### Animal preparation

This study was conducted using five Sprague Dawley male rats (8–12 months old). All experiments were conducted according to the French regulation (Directive 2010/63/EU—French Act Rural Code R 214-87 to 131). The animal facility was approved by veterinarian inspectors (authorization #B 92-032-02) and complies with Standards for Humane Care and Use of Laboratory Animals of the Office of Laboratory Animal Welfare (OLAW—#A5826-01). All experimental procedures were approved by the CEA Ethic Committee (committee #44, approval #10-057). Reporting of this work complies with ARRIVE guidelines. Rats were scanned using a horizontal 11.7 T Bruker scanner (Bruker, Ettlingen, Germany) and a double tuned <sup>1</sup>H-<sup>31</sup>P transmit-receive surface coil (Rapid Biomed GmbH, Rimpfing, Germany). Rats were anesthetized with isoflurane at a concentration kept under 2% to minimize effects on metabolism,<sup>14</sup> and fixed on a stereotaxic frame to minimize motion artifacts.

### Data acquisition

Anatomical images were obtained using a standard T2 sequence and used to position a 10 × 7 × 11 mm<sup>3</sup> voxel covering most of the brain (Figure 1). Localized shimming (~20–25 Hz) was automatically performed after acquisition of a B0 map using the “MAPSHIM” Bruker routine.

Spectroscopic localization was performed using a 3D-ISIS module (TR = 8 s) with 3-ms adiabatic hyperbolic secant inversion pulses (10-kHz bandwidth), and 2-ms adiabatic half passage excitation pulse. In addition to the unsaturated spectrum ( $t_{sat} = 0$ ), spectra were acquired at five different saturation times ( $t_{sat} = 0.53, 1.05, 2.10, 3.15, 4.19$  s). To be less sensitive to B1 inhomogeneity, selective saturation of  $\gamma$ -ATP consisted of a BISTRO pulse train of hyperbolic secant pulses (50-ms each duration, 100-Hz bandwidth)

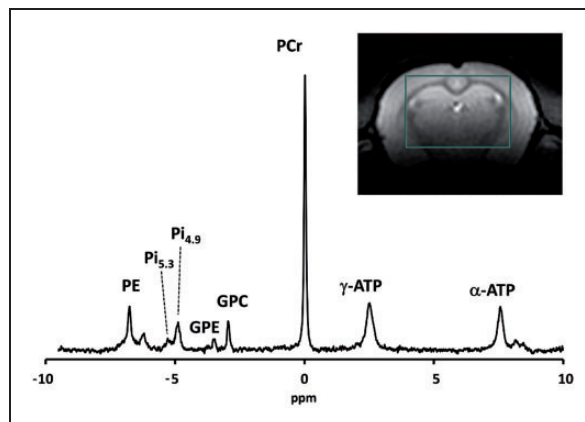


**Figure 1.** Unsaturation <sup>31</sup>P spectra acquired in a large voxel of the rat brain, averaged over two animals, showing different resonances; phosphoethanolamine (PE), the two pools of inorganic phosphate (dominant Pi<sub>4.9</sub>, and newly resolved Pi<sub>5.3</sub>), glycerol 3-phosphorylethanolamine (GPE), glycerol 3-phosphorylcholine (GPC), phosphocreatine (PCr), and ATP resonances (terminal  $\gamma$ -ATP and proximal  $\alpha$ -ATP).

with 5-ms gradient spoiling between pulses.<sup>15</sup> Each spectrum was acquired in 34 min, keeping total examination time under 4 h. To control for direct saturation effects on the spectra, two other rats were scanned using the same protocol with the selective saturation placed symmetrical to  $\gamma$ -ATP resonance relative to Pi, at all  $t_{sat}$ . No detectable signal loss was observed on the dominant Pi peak, demonstrating the absence of significant RF bleed-over effect in our experimental conditions. Hence, in the following, Pi signal attenuations will be calculated relative to the unsaturated spectrum, rather than relative to symmetrically saturated spectra. This approach allows devoting the whole experiment to acquiring “useful” saturation data, i.e. acquire data for more saturation times, and with more averaging.

### Data analysis

Spectra were averaged over all five animals for each  $t_{sat}$  to increase signal-to-noise ratio. This averaged dataset was then analyzed with LCMoDel<sup>16</sup> using a simulated basis set as described in Deelchand et al.<sup>17</sup> Both peaks were visible at the expected Pi resonances, one at 4.9 and the other at 5.3 ppm, and the basis set was built accordingly. The exact chemical shift between each Pi peak and PCr resonance was used to calculate pH in each compartment according to this equation:

$$pH = pKa + \log\left(\frac{\delta - \delta_{ha}}{\delta_a - \delta}\right)$$

Limiting shifts are  $\delta_{\text{ha}} = 3.27$  (acidic species)  $\delta_{\text{a}} = 5.68$  (basic species) and deprotonation constant is  $\text{pK}_{\text{a}} = 6.73$ .<sup>2</sup>

The decrease of Pi longitudinal magnetization during saturation transfer was modeled using Bloch equations modified to account for chemical exchange between Pi and ATP.<sup>18</sup> Non-linear fitting was applied to estimate both  $T1_{\text{int}}$  (the intrinsic T1, in absence of exchange, i.e. during saturation) and  $k_{\text{fATPase}}$  and Monte-Carlo simulations over 500 repetitions was used to derive the error on estimates. Because TR was long as compared with T1, the precise value of  $T1_{\text{mix}}$  (the T1 in presence of exchange, i.e. during sequence dead time) had only marginal impact of  $k_{\text{fATPase}}$ , as we could verify using a complete model including  $T1_{\text{mix}}$ .<sup>18</sup>

## Results

### Amount and pH of Pi pools

Figure 1 shows a localized <sup>31</sup>P spectrum acquired in the rat brain ( $t_{\text{sat}} = 0$ ) with two separate peaks visible around 5 ppm. Each peak is identified with a CRLB of less than 6% and the correlation coefficient between them is weak (0.064). The pH found for each peak was  $\text{pH}_{4.9} = 7.06$  and  $\text{pH}_{5.3} = 7.39$ , respectively. The signal ratio  $\text{Pi}_{5.3}/\text{Pi}_{\text{total}}$  was found to be 19%.

### Progressive saturation

Spectra averaged over five rats and zoomed on the Pi peaks at different saturation times are shown in Figure 2(a). There was no significant decrease of signal intensity for phosphomonoester (PE and PCho) and phosphodiester (GPE and GPC) resonances as  $t_{\text{sat}}$  increased (not shown). The signal decrease of the largest peak at 4.9 ppm reflects the strong chemical exchange between Pi ( $\text{Pi}_{4.9}$ ) and ATP. Figure 2(b) shows the best fit for  $\text{Pi}_{4.9}$  signal attenuation and total Pi attenuation yielding  $k_{\text{fATPase}} = 0.37 \pm 0.03 \text{ s}^{-1}$  and  $k_{\text{fATPase}} = 0.28 \pm 0.02 \text{ s}^{-1}$  for  $\text{Pi}_{4.9}$  and  $\text{Pi}_{\text{total}}$ , respectively. Meanwhile, the signal of alkaline Pi was not apparently affected by progressive saturation (Figure 2(a) and (b)), demonstrating that this pool is not involved in ATP synthesis at detectable levels.

## Discussion

### Extracellular origin of the 5.3 ppm Pi peak

As far as we know, this is the first report of two pools of Pi in the rat brain. To exclude the possibility of an alteration in metabolic profile due to the anesthetic used, e.g. as observed for isoflurane on <sup>1</sup>H spectra (resulting in lactate increase<sup>19</sup>), we acquired control

spectra on a rat anesthetised with benzodiazepine (midazolam) and medetomidine (2.5 and 0.25 mg/kg, respectively). The same peaks in similar concentrations were observed, excluding some metabolic effect due to isoflurane.

Previous studies have reported observing a second Pi peak 0.2–0.4 downfield of the main  $\text{Pi}_{4.9}$  peak in muscles and brain. All studies have excluded the blood contamination possibility, on the basis of small partial volume, low concentration and lack of 2,3-DPG in the spectra. Some reports assign a mitochondrial origin to the second Pi peak in the muscle, with a chemical shift actually closer to 5.1 ppm<sup>8</sup> (and references therein), while others assign an extracellular origin in the brain.<sup>20,21</sup> The different origin of this second Pi in brain<sup>12</sup> compared to muscle<sup>8</sup> is also suggested by the large difference in T1 (approximately four times longer in the brain).

The fact that the  $\text{Pi}_{5.3}$  peak is insensitive to  $\gamma$ -ATP saturation shows that this pool does not participate in *de novo* ATP synthesis at the time scale of the experiment. This was shown here with saturation transfer in the rat brain, and with inversion transfer techniques in the human brain.<sup>12</sup> Using saturation transfer allowed achieving a  $\sim 50\%$  signal decrease for  $\text{Pi}_{4.9}$ , i.e. a much stronger contrast compared to inversion transfer (25% maximal signal decrease). While measurement noise may have partly masked 25% signal attenuation for  $\text{Pi}_{5.3}$  (see Figure 6(a) in Ren et al.<sup>12</sup>), it is less likely that it may have masked a 50%  $\text{Pi}_{5.3}$  decrease in the present work. This strongly reinforces the idea that  $\text{Pi}_{5.3}$  is not in exchange with ATP, thus adding another argument in favor of the extracellular origin of  $\text{Pi}_{5.3}$  in the brain.

Interestingly, we estimated that the extracellular Pi represents 20% of the total Pi in the rat brain, which is close to what has been reported in Ren et al.<sup>12</sup> (35%) and Kintner et al.<sup>20</sup> and Du et al.<sup>21</sup> (25%). Considering that this corresponds well to the generally accepted<sup>22</sup> volume fraction of each of those compartments in the brain, these results suggest that Pi concentrations are similar in the intracellular and extracellular spaces.

### Potential bias on $k_{\text{fATPase}}$ and $V_{\text{ATP}}$ determination

The  $k_{\text{fATPase}}$  value found when modeling only the  $\text{Pi}_{4.9}$  signal is  $\sim 30\%$  higher than when taking the total Pi signal in the voxel. This increase is expected since a higher proportion of the signal considered is in direct exchange with ATP. Remarkably, the values for ATP synthesis rates ( $V_{\text{ATP}} = k_{\text{fATPase}} \times [\text{Pi}]$ ) calculated both ways (considering  $\text{Pi}_{\text{total}}$  or  $\text{Pi}_{4.9}$ ) are very close. This can be explained by the fact that the lower  $k_{\text{fATPase}}$  is multiplied by a higher concentration and vice versa when considering total Pi or dominant Pi only, respectively.

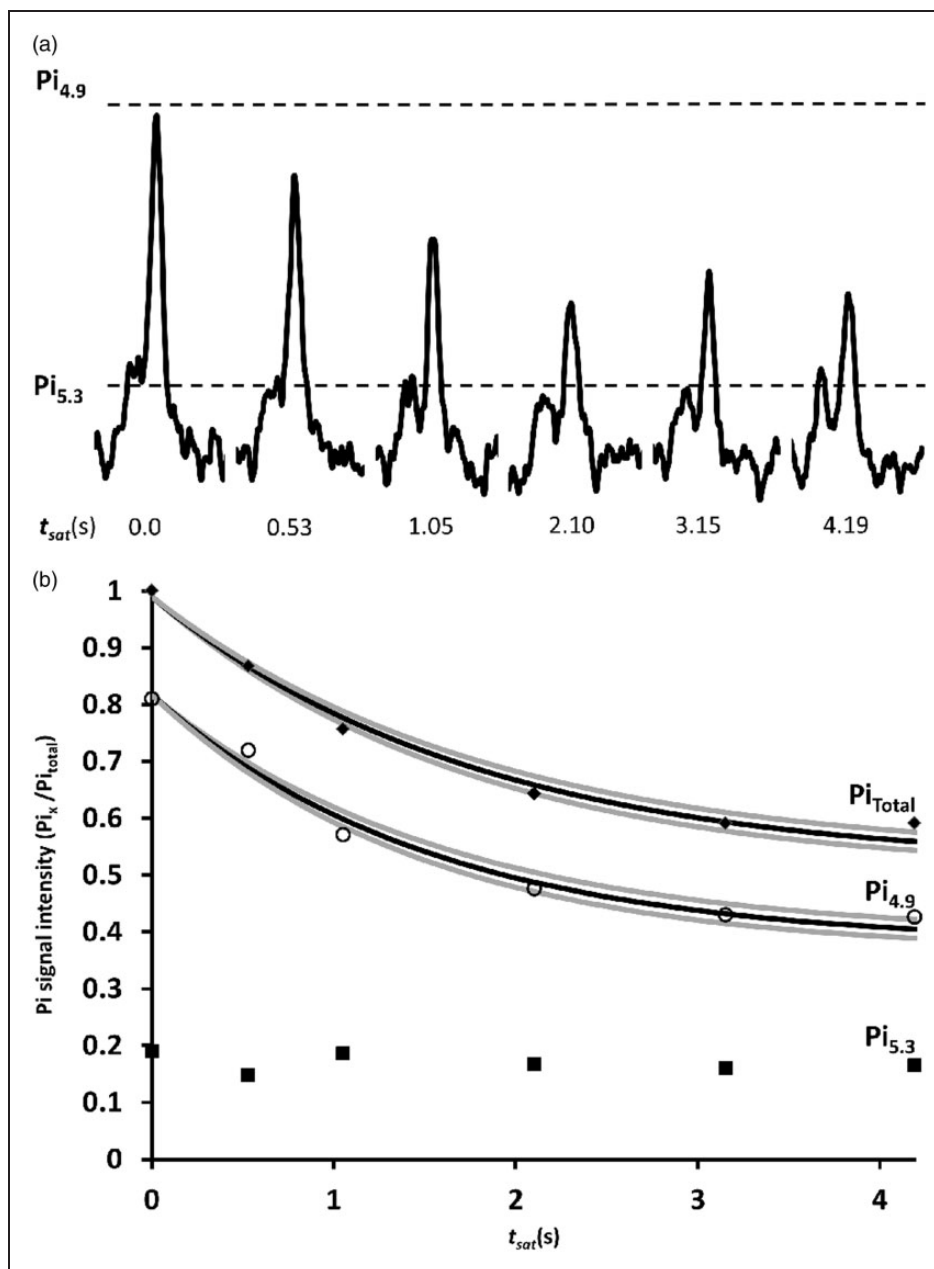


**Figure 2.** (a) Signal decrease of dominant Pi when applying selective saturation on the  $\gamma$ -ATP pool in exchange with Pi. The weaker Pi pool remains unaffected by the downfield saturation suggesting no interaction with  $\gamma$ -ATP. (b) Normalized attenuation of the averaged signal ( $n=5$ ) of total Pi ( $\blacklozenge$ ) and intracellular Pi ( $\circ$ ) as a function of saturation time. The alkaline  $Pi_{5.3}$  ( $\blacksquare$ ) was also plotted to show its independence to  $\gamma$ -ATP saturation. The best nonlinear fit for each  $Pi_{4.9}$  and  $Pi_{total}$  is shown in black line and the uncertainty on  $k_{fATPase}$  is represented as lower and upper bounds in lighter shade.

Using a literature value of 1.3 mM for  $[Pi_{total}]$ , and a 1.1 g/mL brain density,<sup>18,23</sup> ATP synthesis rate can be estimated to  $V_{ATP} = 23.2 \pm 2.2 \mu\text{mol g}^{-1} \text{min}^{-1}$  considering only dominant Pi, and  $V_{ATP} = 22.0 \pm 1.4 \mu\text{mol g}^{-1} \text{min}^{-1}$  considering total Pi. In other words, this means that  $V_{ATP}$  values from past studies based on total Pi attenuation may be essentially correct in practice, despite the presence of extracellular

Pi in the broad peak, while the values of  $k_{fATPase}$  may be significantly underestimated.

Note that estimated  $k_{fATPase}$  and  $V_{ATP}$  values are slightly higher than in previous reports in awake Humans<sup>12,18,21</sup> ( $10.6 \mu\text{mol g}^{-1} \text{min}^{-1}$  on average), macaques under propofol<sup>4</sup> ( $7.8 \mu\text{mol g}^{-1} \text{min}^{-1}$ ), or rats under isoflurane<sup>24</sup> and halothane<sup>25</sup> ( $12.1$  and  $19.8 \mu\text{mol g}^{-1} \text{min}^{-1}$ , respectively). Here, we optimized



the saturation module to neglect RF bleed over and calculate signal attenuation relative to  $t_{\text{sat}}=0$ , rather than relative to symmetric experiment as in previous works. A small RF bleed over, below our detection capabilities, could explain this slight bias towards higher values. This does not affect the findings of the present work regarding the potential bias induced on  $k_{\text{fATPase}}$ , and limited bias on  $V_{\text{ATP}}$  when considering total Pi.

## Conclusion

In this work, we acquired localized  $^{31}\text{P}$  spectra in the rat brain at 11.7 T to characterize a second pool of Pi at more alkaline pH than the main Pi resonance. Based on pH measurements and saturation transfer MRS, we assigned an extracellular origin to this pool and showed that significant bias can be introduced in  $k_{\text{fATPase}}$  measurements when not accounting for both pools. However, this bias does not strongly impact the ATP synthesis rate ( $V_{\text{ATP}}$ ) estimation. Differentiating between intra and extracellular pools may help elucidate some mechanisms at stake under pathological conditions. For example, based on total Pi chemical shift at lower field, we have reported that pH increased in a rat model of Huntington's disease as well as in patients, which we hypothesized to be of intracellular origin.<sup>26</sup> Separating both pools could allow firmly establishing that the observed shift in  $\text{Pi}_{\text{total}}$  is not due to increased extracellular pH or increased  $\text{Pi}_{5,3}$  content, and that only intracellular pH is affected.

## Funding

This work was supported by a grant from Agence Nationale pour la Recherche ("HDeNERGY" project, ANR-14-CE15-0007-01). The 11.7 T MRI scanner was funded by a grant from NeurATRIS: A Translational Research Infrastructure for Biotherapies in Neurosciences ("Investissements d'Avenir," ANR-11-INBS-0011).

## Acknowledgements

We thank Dr Julien Flament, Laura Mouton and Dr Vincent Lebon for the helpful discussions as well as Dr Pierre-Gilles Henry for his technical assistance on configuring LC Model, and Dr Pierrick Jego for help about experimental setup.

## Declaration of Conflicting Interests

The author(s) declared no potential conflicts of interest with respect to the research, authorship, and/or publication of this article.

## Authors' contributions

BT: Experimental design, data acquisition and analysis, data interpretation and manuscript drafting; EM: Data interpretation, critical revision of the manuscript; JV: Experimental

design, data interpretation, critical revision of the manuscript and final approval.

## References

1. Befroy DE, Rothman DL, Petersen KF, et al.  $^{31}\text{P}$ -Magnetization transfer magnetic resonance spectroscopy measurements of in vivo metabolism. *Diabetes* 2012; 61: 2669–2678.
2. De Graaf RA. *In vivo NMR spectroscopy: Principles and techniques*, 2nd ed. Hoboken, NJ: John Wiley & Sons, 2007.
3. Brown TR, Ugurbil K and Shulman RG.  $^{31}\text{P}$  nuclear magnetic resonance measurements of ATPase kinetics in aerobic Escherichia coli cells. *Proc Natl Acad Sci U S A* 1977; 74: 5551–5553.
4. Chaumeil MM, Valette J, Guillemier M, et al. Multimodal neuroimaging provides a highly consistent picture of energy metabolism, validating  $^{31}\text{P}$  MRS for measuring brain ATP synthesis. *Proc Natl Acad Sci U S A* 2009; 106: 3988–3993.
5. Wary C, Naulet T, Thibaud J-L, et al. Splitting of Pi and other  $^{31}\text{P}$  NMR anomalies of skeletal muscle metabolites in canine muscular dystrophy. *NMR Biomed* 2012; 25: 1160–1169.
6. Schmidt O, Bunse M, Dietze GJ, et al. Unveiling extracellular inorganic phosphate signals from blood in human cardiac  $^{31}\text{P}$  NMR spectra. *J Cardiovasc Magn Reson* 2001; 3: 325–329.
7. Garlick PB, Soboll S and Bullock GR. Evidence that mitochondrial phosphate is visible in  $^{31}\text{P}$  NMR spectra of isolated, perfused rat hearts. *NMR Biomed* 1992; 5: 29–36.
8. Kan HE, Klomp DWJ, Wong CS, et al. In vivo  $^{31}\text{P}$  MRS detection of an alkaline inorganic phosphate pool with short T1 in human resting skeletal muscle. *NMR Biomed* 2010; 23: 995–1000.
9. Fitzpatrick JH, Kintner D, Anderson M, et al. NMR studies of Pi-containing extracellular and cytoplasmic compartments in brain. *J Neurochem* 1996; 66: 2612–2620.
10. Gilboe DD, Kintner D, Anderson ME, et al. Inorganic phosphate compartmentation in the normal isolated canine brain. *J Neurochem* 1993; 60: 2192–2203.
11. Gilboe DD, Kintner DB, Anderson ME, et al. NMR-based identification of intra- and extracellular compartments of the brain Pi peak. *J Neurochem* 2002; 71: 2542–2548.
12. Ren J, Sherry AD and Malloy CR.  $(^{31}\text{P})\text{P}$ -MRS of healthy human brain: ATP synthesis, metabolite concentrations, pH, and T1 relaxation times. *NMR Biomed* 2015; 28: 1455–1462.
13. Ren J, Sherry AD and Malloy CR. Amplification of the effects of magnetization exchange by  $^{31}\text{P}$  band inversion for measuring adenosine triphosphate synthesis rates in human skeletal muscle. *Magn Reson Med* 2014; 74: 1505–1514.
14. Bresnen A and Duong TQ. Brain high-energy phosphates and creatine kinase synthesis rate under graded isoflurane

- anesthesia: an in vivo  $(31)P$  magnetization transfer study at 11.7 tesla. *Magn Reson Med* 2014; 73: 726–730.
15. Luo Y, de Graaf RA, DelaBarre L, et al. BISTRO: an outer-volume suppression method that tolerates RF field inhomogeneity. *Magn Reson Med* 2001; 45: 1095–1102.
  16. Provencher SW. Automatic quantitation of localized in vivo  $1H$  spectra with LCModel. *NMR Biomed* 2001; 14: 260–264.
  17. Deelchand DK, Nguyen T-M, Zhu X-H, et al. Quantification of in vivo  $31P$  NMR brain spectra using LCModel. *NMR Biomed* 2015; 28: 633–641.
  18. Lei H, Ugurbil K and Chen W. Measurement of unidirectional  $P_i$  to ATP flux in human visual cortex at 7 T by using in vivo  $31P$  magnetic resonance spectroscopy. *Proc Natl Acad Sci U S A* 2003; 100: 14409–14414.
  19. Boretius S, Tammer R, Michaelis T, et al. Halogenated volatile anesthetics alter brain metabolism as revealed by proton magnetic resonance spectroscopy of mice in vivo. *Neuroimage* 2013; 69: 244–255.
  20. Kintner DB, Anderson ME, Sailor KA, et al. In vivo microdialysis of 2-deoxyglucose 6-phosphate into brain. *J Neurochem* 2002; 72: 405–412.
  21. Du F, Zhu X-H, Qiao H, et al. Efficient in vivo  $31P$  magnetization transfer approach for noninvasively determining multiple kinetic parameters and metabolic fluxes of ATP metabolism in the human brain. *Magn Reson Med* 2007; 57: 103–114.
  22. Syková E and Nicholson C. Diffusion in brain extracellular space. *Physiol Rev* 2009; 88: 1277–1340.
  23. Jensen JE, Drost DJ, Menon RS, et al. In vivo brain  $(31)P$ -MRS: measuring the phospholipid resonances at 4 Tesla from small voxels. *NMR Biomed* 2002; 15: 338–347.
  24. Du F, Zhu X-H, Zhang Y, et al. Tightly coupled brain activity and cerebral ATP metabolic rate. *Proc Natl Acad Sci U S A* 2008; 105: 6409–6414.
  25. Shoubridge EA, Briggs RW and Radda GK.  $31P$  NMR saturation transfer measurements of the steady state rates of creatine kinase and ATP synthetase in the rat brain. *FEBS Lett* 1982; 140: 288–292.
  26. Chaumeil MM, Valette J, Baligand C, et al. pH as a biomarker of neurodegeneration in Huntington's disease: a translational rodent-human MRS study. *J Cereb Blood Flow Metab* 2012; 32: 771–779.